Biochimica et Biophysica Acta 1858 (2016) 97–103

Contents lists available at ScienceDirect

Biochimica et Biophysica Acta

journal homepage: www.elsevier.com/locate/bbamem

The biophysical properties of ethanolamine plasmalogens revealed by atomistic molecular dynamics simulations

Tomasz Rog [a], Artturi Koivuniemi [b,*]

[a] Department of Physics, Tampere University of Technology, Tampere, Finland
[b] VTT Technical Research Center of Finland, Espoo, Finland

ARTICLE INFO

Article history:
Received 26 June 2015
Received in revised form 27 October 2015
Accepted 28 October 2015
Available online 30 October 2015

Keywords:
Lipid membrane
Plasmalogens
Neurodegenerative diseases
Molecular dynamics

ABSTRACT

Given the importance of plasmalogens in cellular membranes and neurodegenerative diseases, a better understanding of how plasmalogens affect the lipid membrane properties is needed. Here we carried out molecular dynamics simulations to study a lipid membrane comprised of ethanolamine plasmalogens (PE–plasmalogens). We compared the results to the PE–diacyl counterpart and palmitoyl-oleyl-phosphatidylcholine (POPC) bilayers. Results show that PE–plasmalogens form more compressed, thicker, and rigid lipid bilayers in comparison with the PE–diacyl and POPC membranes. The results also point out that the vinyl–ether linkage increases the ordering of sn-1 chain substantially and the ordering of the sn-2 chain to a minor extent. Further, the vinyl–ether linkage changes the orientation of the lipid head group, but it does not cause changes in the head group and glycerol backbone tilt angles with respect to the bilayer normal. The vinyl–ether linkage also packs the proximal regions of the sn-1 and sn-2 chains more closely together which also decreases the distance between the rest of the sn-1 and sn-2 chains.

1. Introduction

Plasmalogens are a special subclass of glycerophospholipids that are characterized by the presence of a vinyl–ether linkage at the sn-1 position, and an ester linkage at the sn-2 position. Plasmalogens are found in nearly all animal and anaerobic bacterial cells [1], and they constitute 15–20 mol% of total phospholipids in the cell membranes [2,3]. Furthermore, plasmalogens are also found in subcellular membranes as well as in specialized membranes such as myelin and synaptic vesicles [3,4]. Interestingly, plasmalogen ethanolamines (PlsEtn) constitute up to 85 mol% of total phosphatidylethanolamine (PE) species and up to 30 mol% of total phospholipids in nerve tissue membranes [3].

The role of plasmalogens in cell membranes has aroused scientists' interest for decades since it has been found that the amount of plasmalogens is reduced in various neurodegenerative disorders, such as Zellweger syndrome (ZS), Alzheimer's disease (AD), and Down syndrome (DS) [3,5]. In the case of AD and DS the reason for the reduction of plasmalogens is poorly understood, but in the case of ZS a plasmalogen deficit is a direct consequence of the genetic defect.

For instance, patients suffering from Alzheimer's disease (AD) have been shown to have decreased levels of plasmalogens in brain areas that are under degeneration, and the extent of reduction correlates with the severity of the disease [3,6]. Because plasmalogens are important constituents of various lipid membrane structures and their central role in different human disorders, it is essential to determine their biophysical properties and what kind of changes these features exert on lipid membrane structure and dynamics, as well as on the function of membrane proteins. In this way, new information will be discovered leading to a comprehensive understanding of the processes mediated by plasmalogens.

Concerning the biophysical properties of plasmalogens, experiments have demonstrated that plasmalogens have lower lamellar gel to liquid-crystalline and lamellar to inverse-hexagonal phase transition temperatures compared to alky and diacyl counterparts [7–9]. Moreover, the plasmalogen-deficient cells derived from patients affected with the Zellweger syndrome (plasmalogen content 0–5% of total phospholipids) showed lower fluorescence anisotropies corresponding to higher membrane fluidity and decreased order compared to the controls (plasmalogen content 13–15%), suggesting that plasmalogens rigidify biological membranes [10]. Further, since ethanolamine plasmalogens have a stronger tendency to promote the formation of inverted hexagonal phases, they are suggested to facilitate membrane fusion events in different contexts [5]. However, the sub-molecular details behind the above properties are not fully understood, although NMR spectroscopy measurements have suggested that the vinyl–ether linkage at the sn-1 position induces a conformational change to the glycerol backbone driving the closer packing of the sn-1 and sn-2 chains at the proximal region

* Corresponding author.
E-mail address: artturi.koivuniemi@vtt.fi (A. Koivuniemi).

http://dx.doi.org/10.1016/j.bbamem.2015.10.023

[11]. This in turn induces a closer packing of lipids at the water–lipid interface, which may promote the formation of the inverted hexagonal phase by reducing the area taken by the lipid head group. Further, it was shown that the orientation of the polar head group with respect to the membrane surface differs between choline plasmalogens and diacyl phosphatidylcholine [12].

Aside from the importance of plasmalogens on the structural features of lipid membranes, they are important antioxidant agents and lipid mediators. Since the vinyl–ether bond is highly sensitive to oxidative attack compared to their ester counterparts, it has been suggested that plasmalogens act as molecular scavengers, protecting cells and especially lipids from oxidative damage [13]. Furthermore, as plasmalogens often contain arachidonic acid (AA) or docosahexaenoic acid (DHA) at the sn-2 position, they are important in the synthesis of eicosanoids and in the signal transduction processes via plasmalogen-selective-PLA2-mediated release of DHA and AA [14].

In the present study, our aim is to clarify the molecular properties of ethanolamine plasmalogens (PE–plasmalogen) and especially the role of vinyl–ether linkage utilizing atomistic molecular dynamics simulations. Thus, we simulated three bilayers systems comprised of either PE–plasmalogen PE–diacyl, or POPC lipid species. The results revealed that PE–plasmalogens lipids form more condensed and rigid bilayers compared to their diacyl counterparts and POPCs. These features were influenced by the vinyl–ether linkage due to its marked effects on the properties of the sn-1 and sn-2 chains.

2. Materials and methods

2.1. Simulated systems

In this study, three different lipid bilayer systems were studied: a PE–plasmalogen bilayer system (P-16:0/20:4), a PE–diacyl bilayer system (16:0/20:4) and a POPC bilayer system (16:0/18:1). According to the literature, PE(P-16:0/20:4) is not decreasing during AD [3]. However, it has been found that the reduction of PE(P-16:0/20:4) correlates with severity of AD related cognitive impairment although it does not correlate with post-mortem AD pathology [15]. The diacyl counterpart system was chosen in order to reveal the effect of the vinyl–ether linkage on the properties of plasmalogens. The POPC bilayer was chosen for comparison purposes because it is one of the most abundant lipid species in biological membranes and because it is experimentally as well as computationally well characterized. Each lipid bilayer system consisted of 128 lipid and 3500 water molecules. The chemical structures for the simulated lipid species are shown in Fig. 1.

2.2. Force field and simulation parameters

To parameterize lipid molecules, the OPLS-AA (Optimized Potentials for Liquid Simulations-All Atom) force field was used with recently derived parameters for the long hydrocarbons, glycerol backbone and head group (so-called MACROG lipids) [16]. For unsaturated lipids, a

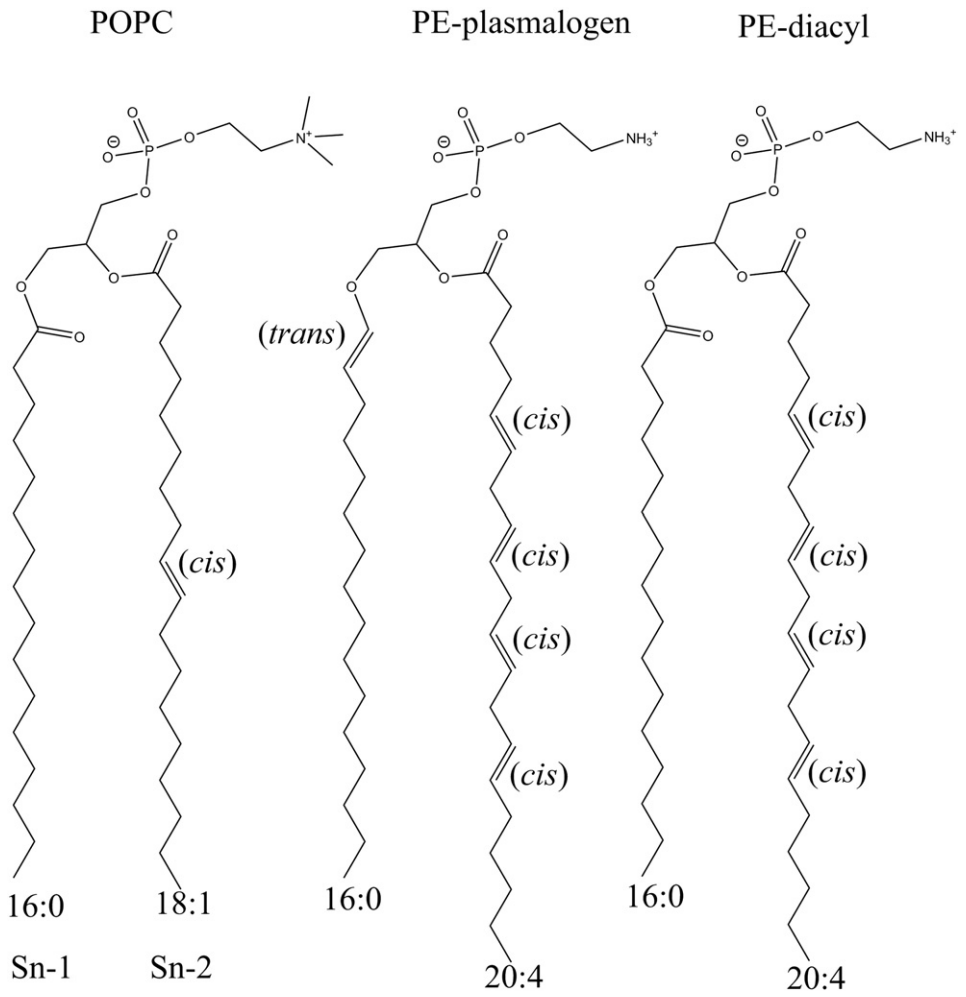

Fig. 1. The chemical structures for the POPC, PE–plasmalogen, and PE–diacyl lipid species. The chain lengths and saturation degree of the sn-1 and sn-2 chains are marked below the chemical structures.

new set of parameter was also derived [17]. For the vinyl bond, we used the original OPLS parameters. The TIP3P force field was used to handle water molecules [16,18]. The cut-off for the Lennard–Jones potential was set to 1 nm. The Particle Mesh Ewald summation method with a real space cut-off of 1 nm was utilized in the calculation of electrostatic interactions [19]. The Verlet cut-off scheme was employed [20]. The simulation temperature and pressure were set to 310 K and 1 bar, respectively. The Nose–Hoover thermostat [21,22] and the Parrinello–Rahman barostat [23] coupling schemes were employed with the coupling constants of 0.1 and 1.0 ps^{-1}. The simulated systems were run until a 200 ns long trajectory was produced, from which the last 100 ns was used in the analysis. The simulations were performed with the GROMACS 4.6.5 simulation package [24] and carried out with a desktop computer with Intel Core i7-3930 K processor and Nvidia GeForce 970 graphical processing unit.

2.3. Analysis

For the density profile calculations, we used the g_density program included in the GROMACS package. To construct a density profile for the each lipid bilayer system, the simulation box was divided into 50 slices along the bilayer normal. The atom densities were calculated in each slice and averaged over all simulation frames. The g_hbond program was used with the default parameters to calculate the hydrogen bonds between water and glycerol backbone oxygens.

Lipid head group and acyl chain deuterium order parameters were calculated from the trajectories by using the following relation:

$$|S_n| = \frac{3}{2}<cos^2\theta_n> - \frac{1}{2}, \quad (1)$$

where θ_n is the angle between the vector from the carbon n to the hydrogen attached to the carbon n and the normal of the bilayer.

The conformations of lipid head group and glycerol backbone with respect to the normal of the bilayer were calculated by utilizing an in-house written program. The g_dist program of GROMACS package was used to calculate the distances between the equivalent carbons in the sn-1 and sn-2 acyl chains.

The errors were estimated by using a block averaging technique. The last 100 ns of simulation trajectory was divided to five blocks whose averages were determined in respect of the quantity of interest. The block averages were then used to determine the standard deviations for the different quantities.

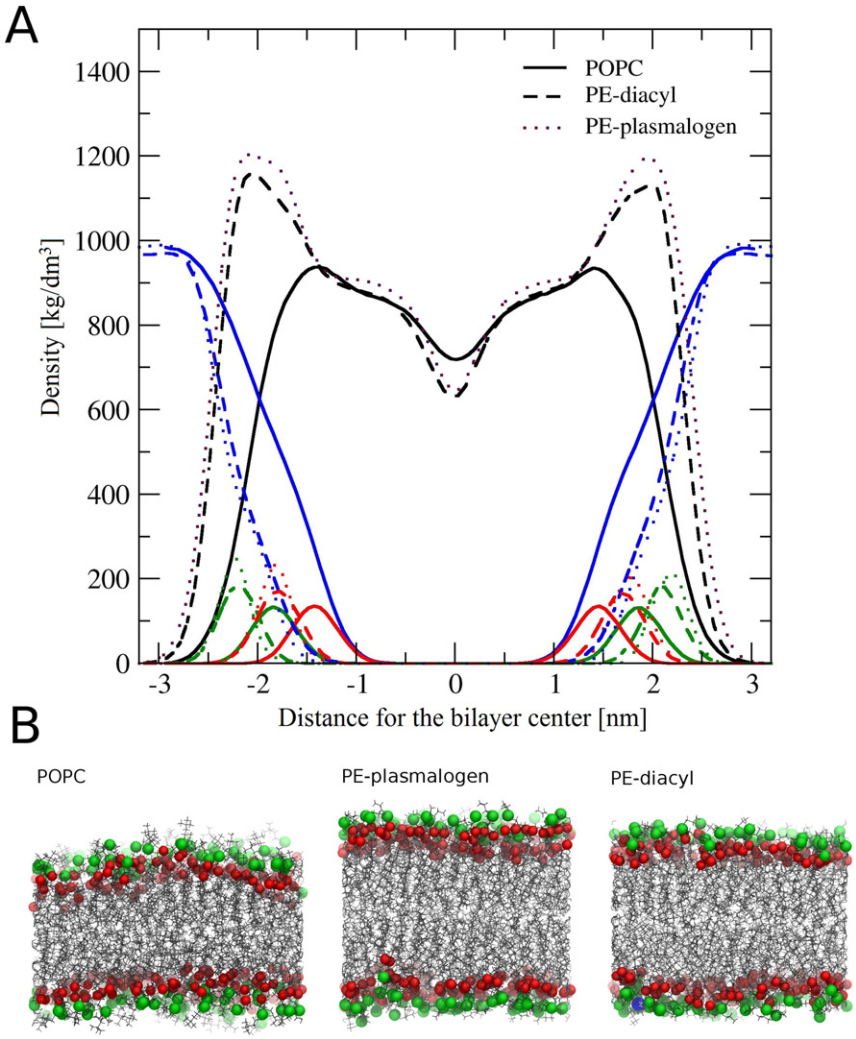

Fig. 2. Density profiles and simulation snapshots for each simulated system. (A) The density profiles for the lipid bilayer systems where whole lipid molecules are marked in black, water in blue, the phosphorous atoms of lipids in green, and the ester/ether oxygen atoms of lipids in red color. (B) Snapshot from the end of simulations. The coloring is the same as in the case of density profiles. The acyl chains of lipids are rendered using sticks, the phosphorous and ester/ether oxygen atoms are rendered as van der Waals spheres.

3. Results and discussion

3.1. The vinyl–ether linkage compresses lipid bilayers

The density profiles and simulation snapshots in Fig. 2 reveal that PE–plasmalogens form thicker and more condensed lipid bilayers compared to the POPC and PE–diacyl lipid bilayers. We used the average distance between phosphorous atoms of the opposing bilayer leaflets to estimate the thicknesses of lipid bilayers in each case. The bilayer thickness for the POPC, PE–plasmalogen, and PE–diacyl bilayers were determined to be 3.7 ± 0.1 nm, 4.4 ± 0.1 nm, 4.2 ± 0.1 nm, respectively. Thus, the PE–plasmalogen bilayer is approximately 1 nm thicker compared to the POPC bilayer. According to the results, the vinyl–ether linkage alone increases the thickness of the bilayer by ~0.2 nm. Interestingly, the PE–plasmalogen and PE–diacyl lipid bilayers are much more condensed (larger density peaks) in the head group regions compared to the POPC bilayer. The results indicate that the presence of the vinyl–ether bond leads to a slightly more compressed bilayer. There is also a slight density decrease in the middle of the PE–plasmalogen and PE–diacyl bilayers compared to the POPC system. This decrease, however, is small compared to the density changes seen in the head group region. Thus, based on the density profiles only, PE–plasmalogens form more compressed bilayers compared to POPCs, and this is largely because of the PE head group.

In order to get a better view concerning the water penetration to the different lipid bilayers, we also estimated the relative amount of water in the glycerol region of lipids by calculating the average number of hydrogen bonds formed between water and ester oxygens (data not shown). The results showed that the in the PE–lipid systems water molecules form ~30% less hydrogen bonds with the glycerol oxygens compared to the POPC system.

Next, we determined the area per lipid for each system to further verify the condensation trend seen in the density profiles. This was carried out by dividing the average bilayer area by the number of lipids in one leaflet. For the PE–plasmalogen system, the area per lipid was 0.53 ± 0.01 nm^2; for the POPC system 0.68 ± 0.01 nm^2; and for the PE–diacyl system 0.58 ± 0.01 nm^2. For comparison purposes, the previously simulated area per lipid for 1-palmitoyl-2-oleoyl-sn-glycero-3-phosphoethanolamine (POPE, 16:0/18:1) and 1-palmitoyl-2-arachidonoyl-sn-glycero-3-phosphocholine (PAPC, 16:0/20:4) bilayers were ~0.55 nm^2 and ~0.70 nm^2 indicating that by changing PC head group to PE, or oleate fatty acid (18:1) to arachidonic acid (20:4) should decrease and increase the area per lipid by ~0.12 nm^2 and ~0.02 nm^2, respectively [25]. Thus, in light of this the area per lipid values reported for the simulated systems seems reasonable. However, the effect of PE head group to the area per lipid could vary depending on the length and unsaturation of acyl chains.

The area per lipid results agree with our interpretations based on the density profiles, indicating that PE–plasmalogen lipids pack together more closely. Interestingly, the area per lipid calculations revealed that the vinyl–ether linkage plays an important role in the lipid packing since its contribution to the area per lipid was ~0.06 nm^2. Our results are consistent with the monolayer experiments carried out by Smaby et al. revealing a smaller cross-sectional area for choline plasmalogen compared to its diacyl analog [26].

One explanation for the lower area per lipid of the PE–plasmalogen system compared to the PE–diacyl system could be the finding that water molecules are able to form fewer number of hydrogen bonds with the vinyl–ether linkages compared to the ester linkages. Interestingly, the vinyl–ether linkage has been shown to decrease the lamellar-to-inverse-hexagonal-phase transition temperature by 10–20° [7]. The lamellar-to-inverse-hexagonal-phase transition temperature is determined by the ability of the lipid bilayers to form negatively curved lipid phases which is influenced by the spontaneous curvature of the bilayer [25]. Although we did not calculate the spontaneous curvatures for the simulated bilayer systems, we can predict and speculate based on the simulated derived density profiles that the PE–plasmalogen bilayer has a more negative spontaneous curvature compared to the POPC bilayer. This is because the packing of head group regions in the PE–plasmalogen system was registered to be much higher compared to the POPC system.

In conclusion, our results point out that the PE head group (in accordance with previous studies) and the vinyl–ether linkage of the sn-1 chain in plasmalogens are behind the increased packing and thickness of the plasmalogen bilayer studied here. Further, the packing is predominantly taking place at the head group region suggesting that the negative spontaneous curvature increases simultaneously.

3.2. The vinyl–ether linkage increases the ordering of sn-1 and sn-2 chains

Next, we analyzed the deuterium order parameters for the sn-1 and the sn-2 chains in the POPC, PE–plasmalogen and PE–diacyl systems. Fig. 3 reveals that the sn-1 chain is more ordered in the PE–lipid systems when compared to the POPC system. Interestingly, the sn-2 chain of PE–lipids is substantially more disordered at the beginning of the chain (carbons 4–7), but at the end of the chain some of the hydrogens are more ordered compared to POPC (carbons 17–19). In addition, it is clear that the presence of vinyl–ether linkage induces higher ordering of the sn-1 chain. Concerning the sn-2 chain, a similar effect is registered, although the effect is slightly smaller. The sn-2 chain of POPC was expected to be more ordered compared to the PE–lipids, since the sn-2 chain of POPC contains only one double, whereas in the case of PE–lipids the sn-2 chain is polyunsaturated (four double bonds). Taken together, we can safely claim that the PE–lipid species studied here form less fluid lipid bilayers compared to POPC, and the vinyl–ether linkage has the ability to increase the rigidity of lipid acyl chains studied here. However, the reason why the vinyl–ether linkage induces a higher acyl chain order is not yet understood.

Our results agree with the previous experimental findings showing that plasmalogen-depleted cellular membranes are more fluidic compared to the controls [10]. However, the results seem to be inconsistent with the fact that the introduction of vinyl–ether linkage to a lipid structure lowers its lamellar-gel-to-liquid-crystalline-phase transition temperatures by 6–10° [7,8]. However, one must remember that the lamellar-gel-to-liquid-crystalline-phase transition temperature is also affected by other features, and not just by the rigidness of the acyl chains. It is possible that the addition of vinyl–ether linkage decreases

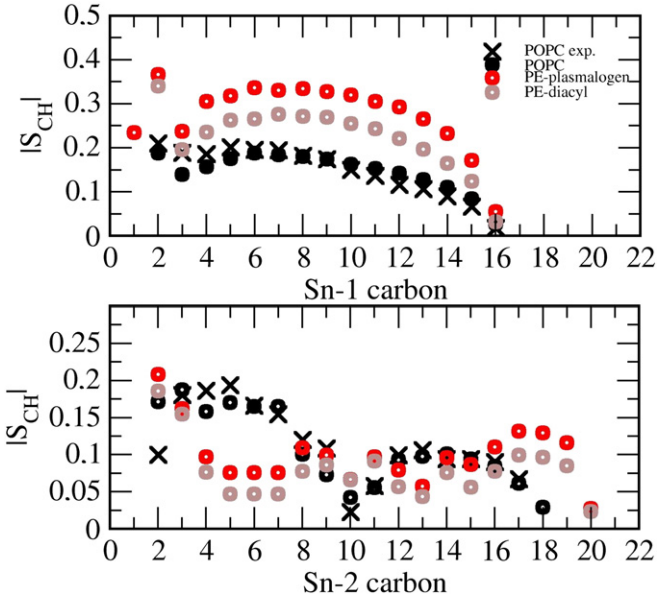

Fig. 3. Deuterium order parameters for the sn-1 and sn-2 chains as a function of acyl chain carbons. (top) The order parameters for the sn-1 chains. (bottom) The order parameters for the sn-2 chains. The errors are about the size of the markings.

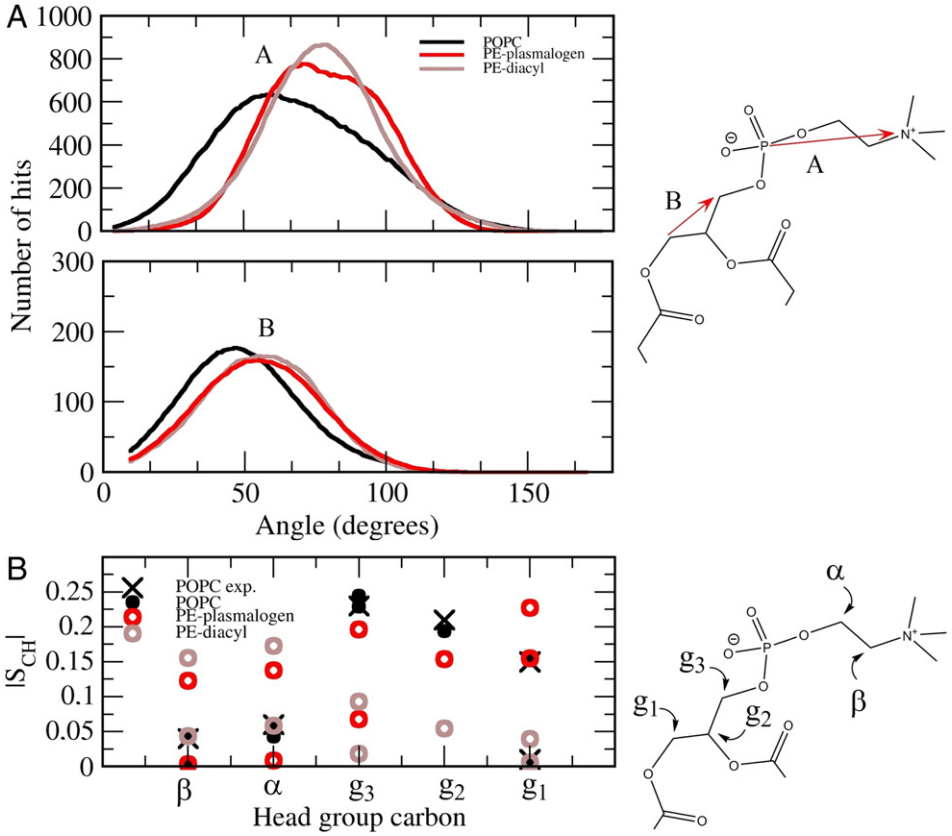

Fig. 4. (A) The lipid head group and glycerol backbone orientations with respect to the bilayer normal. The vectors used in the analysis are shown on the right. (B) The lipid head group order parameters for the β, α, g1, g2 and g3 carbon hydrogens. The head group carbons analysed are shown in the right. The errors are about the size of the markings.

the attraction of adjacent lipids by several mechanisms such as disrupting the optimal glycerol backbone interactions or changing the orientation of lipids with respect to each other.

3.3. The vinyl–ether linkage induces a conformational rearrangement to the lipid head group

The head group angle distribution profiles and deuterium order parameters in Fig. 4 show clear differences in the head group orientations between the simulated lipid systems. Based on angle distributions, the PE–lipids have more tilted orientations compared to POPCs (top). The PE–plasmalogen system shows a slightly blunted angle distribution when compared with the PE–diacyl system. These results are not surprising since it is well known that when the choline head group is changed to the ethanolamine one, the head group tilts more toward the plane of the lipid bilayer because the ethanolamine hydrogens readily form hydrogen bonds with the oxygen atoms of phosphate groups [27].

Interestingly, the head group deuterium order parameters show differences in the head group conformations between the PE species that are not noticeable from the angle distributions (see Fig. 4 bottom). More specifically, PE head group induces non-equal hydrogen order parameters for β-, α-, g3- and g1-carbons, which is not seen in the case of the POPC system. The vinyl–ether linkage also induces non-equal hydrogen order parameters for β-, α-, g3- and g1-carbons, but the hydrogen order parameters of β- and α-carbon are lower compared to the PE–diacyl system. In contrast to α- and β-carbon hydrogens, the vinyl ether linkage increases the ordering of g3-, g2- and g1-carbon hydrogens.

Our results concerning the head group order parameters of POPC agree well with the experimental results, providing support that our atomistic force field should be reasonably accurate for probing the effect of different chemical groups to the orientation of lipid head groups [28]. According to the proton NMR measurements carried out by Han et al. the orientation of head group is different between plasmenylcholines and phoshatidylcholines [11]. This was further supported by the following proton NMR studies measuring the chemical and magnetic inequivalence of the methylene and methine protons of glycerol backbone [29]. More specifically, the two diastereotopic sn-3 methylene protons of the glycerol backbone in the vinyl–ether linked phospholipids are chemically and magnetically more inequivalent than the comparable protons present in ester linked phospholipids. In contrast, the two sn-1 diastereotopic methylene protons are more equivalent in vinyl–ether linked phospholipids compared to ester linked phospholipids. In addition, according to experiments the sn-2 methine proton is more shielded in vinyl–ether linked phospholipids. Analysis of these experiments and subsequent computer simulations revealed that rather modest chemical alterations at the sn-1 chain can cause changes in the distribution of the conformational states of the glycerol backbone that induce a more perpendicular orientation of choline plasmalogen head group with respect to the membrane surface when compared to diacyl phosphatidylcholines. The more perpendicular head group orientation was also suggested for lysoplasmenylcholine based on fluorescence spectroscopy measurements [9]. These results support our simulation results by a moderate amount since spatially non-equal sn-3 (g3) protons were registered in the PE–plasmalogen system whereas in the case of POPC the sn-3 protons are spatially equivalent. Further, the spatial equivalence of sn-1 (g1) protons is higher in the PE–plasmalogen system. Similar kind of behaviour was also registered in the PE–diacyl system suggesting that the PE head group could also induce conformational arrangements to glycerol backbone. However, the proton NMR parameters measured by Han et al. cannot be directly compared to the deuterium order parameters, since the proton NMR results are mostly affected by the chemical structure and surrounding functional groups

whereas the deuterium order parameters give information from the average orientation of C—H bonds with respect to the bilayer normal. In addition, the deuterium NMR measurements of Gally et al. indicate that the glycerophospholipids, independent of their specific chemical structure, are characterized by a unique average glycerol backbone conformation [30]. In other words, the glycerol backbone conformation should not be altered by the lipid head group (when PC is replaced by PE). In contrast, our simulation results here suggest that the deuterium order parameters of glycerol backbone are different in the POPC and PE–diacyl systems. The differences between our simulations and experiments may be due to the different acyl chains in the systems or possible limitations in the used force field parameters. The limitations of the current lipid force fields regarding the lipid head group order parameters are discussed in detail in the paper of Botan et al. [31] Nevertheless, the effects of PE head group and the vinyl–ether bond on the head group orientation presented in this study can be validated and further scrutinized by NMR measurements in the future.

3.4. The vinyl–ether linkage packs the proximal regions of the sn-1 and sn-2 chains more closely together

To verify the previously predicted feature that the vinyl–ether linkage brings the proximal regions of the sn-1 and sn-2 chains closer together, we calculated distances for carbon pairs formed by the equivalent sn-1 and sn-2 acyl chain carbons (see Fig. 5.) Results indicate that the vinyl–ether linkage induces a closer packing of the sn-1 and sn-2 acyl chains, and this is mainly due to the distance minimum seen in the distance profile of the PE–plasmalogen system. In other words, the distance trend of PE–plasmalogen slightly decreases when moving from the carbon pair one to the pair two, whereas, in the case of the POPC and PE–diacyl systems, the same distance trend is increasing. Further, results point out that distances are approximately same for the carbon pairs one, two, three and four in the PE–plasmalogen system.

Our simulation results are in agreement with the previous NMR measurements of Han et al. who demonstrated that the proximal regions of sn-1 and sn-2 aliphatic chains were closer to each other when the ester linkage was replaced by the vinyl–ether linkage [11]. They also concluded based on the distance restraints that the carbon atoms which comprise the proximal portion of the sn-2 aliphatic chain in plasmenylcholine are nearly coplanar and parallel to the sn-1 aliphatic chain. The simulation results here agree with this view since the carbon pair distances stay more or less the same up to the carbon pair four. A probable reason for this is that the distance of carbon pair two is ~0.1 nm less in the PE–plasmalogen system compared to the other simulated lipid systems. After the carbon pair two the distance profile of PE–plasmalogen system behaves similarly compared to the PE–diacyl system. The carbon two in the vinyl–ether linked sn-1 chain is the last carbon atom which is part of the planar structure generated by the *trans* double bond (Z-double bond) of vinyl–ether linkage, meaning that starting from the carbon three the sn-1 chain can jump freely between different rotamer conformations. The above experimental and simulation results are in agreement with the view based on experimental data that the Z-double bonds are essentially aligned parallel to bilayer normal [32].

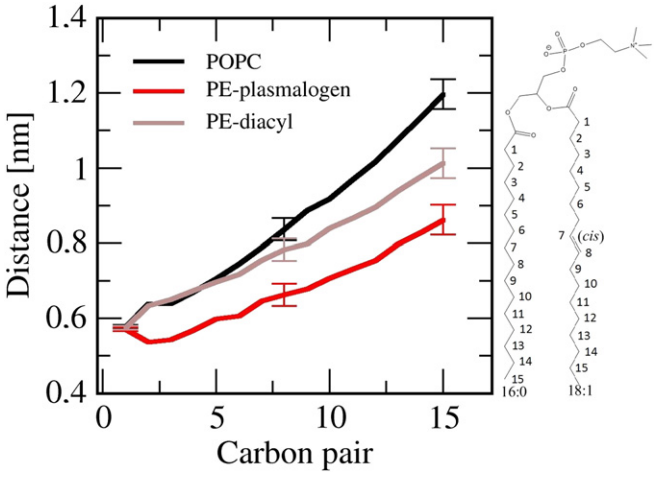

Fig. 5. The distances for the carbon pairs formed by the equivalent carbons of sn1- and sn-2 acyl chains. The carbon pairs are marked with numbers to the chemical structure of POPC displayed on the right.

In conclusion, regarding the area per lipid and acyl chain order parameters results above, the vinyl–ether linkage induced closer packing of sn-1 and sn-2 chains explains the lower area per lipid and higher acyl chain ordering of the PE–plasmalogen system compared to the PE–diacyl system.

4. Conclusions

Given the relevance of plasmalogen depletion in several neurodegenerative diseases, it is important to understand how plasmalogens modulate the biophysical features of lipid membranes. Thus, here we have studied three different lipid systems with atomistic molecular dynamics simulations to reveal the molecular characteristics of PE–plasmalogen bilayer (16:0;20:4), and especially the role of vinyl–ether linkage. We analyzed how the bilayer thickness, lipid acyl chain ordering and head group orientation differ between the studied systems.

In the present study, we have demonstrated that plasmalogens form more condensed and thicker lipid bilayers when compared to the POPC or the corresponding diacyl system. Furthermore, our work showed that the vinyl–ether linkage of plasmalogens markedly increases the condensation of a lipid bilayer. The increased thickness and decreased area per lipid were accompanied with a higher ordering of the sn-1 acyl chain. Surprisingly, the absence of vinyl–ether linkage did not change the head group or the glycerol backbone angle distribution with respect to the bilayer normal. However, the head group deuterium order parameters were influenced by the presence of vinyl–ether linkage, pointing out that the vinyl–ether linkage induces a conformational shift to the head group, which is not registered in the head group angle or glycerol backbone angle profiles. To verify the previous experimental findings regarding the orientation of the proximal regions of the sn-1 and sn-2 chains in vinyl–ether linked plasmalogens, we analyzed the carbon–carbon distances formed by the sn-1 and sn-2 chains. Our results show, in agreement with experiments, that the vinyl–ether linkage packs the proximal regions of acyl chains closer together as well as the rest of the acyl chains. The aforementioned lipid membrane properties are important in the proper functioning of biological membranes. For example the thickness and fluidity affects the permeability of small molecules through the membrane [33]. In addition the cell membrane thickness has been shown to modulate the sorting, aggregation and function of cell membrane proteins and lipids [34].

Considering the above, it is not perhaps a surprise that plasmalogens are enriched in the mammalian brain, because in the nerve cells and myelin sheath the plasma membrane leakage is probably more tightly controlled compared to other cell types in order to maintain the proper ion gradient across the plasma membrane, which is crucial for an effective nervous system function. In addition to passage of small molecules, plasmalogens form inverted hexagonal phases in the physiological temperatures which likely has a facilitating contribution to the formation and fusion of synaptic vesicles. Further, the higher lipid membrane condensation and thickness induced by plasmalogens could contribute to the membrane protein function and to the attachment of small proteins and peptides to the lipid membrane surface which could increase the porousness of the cell membrane. For example, Winkler and coworkers have demonstrated that the generation of Alzheimer's disease-associated amyloid β42/43 peptide by γ-secretase depends on the lipid membrane thickness [35].

In the future it would be interesting to reveal how much plasmalogen levels are actually able to change the biophysical properties of native lipid membranes where a mixture of different lipid species exists. Even though real biological membranes are much more complex the effect of plasmalogens to lipid membrane properties can be substantial since in average 10–20 mol% of total phospholipids are plasmalogens, and even up to 30 mol% of total phospholipids in nerve tissue membranes are plasmalogens. For example, if the plasmalogen content reduces from 20 to 10 mol% of the total phospholipids, it could reduce e.g. the thickness and increase the fluidity of a plasma membrane. In addition, it is plausible that the effect of reduction would be more pronounced if plasmalogens are concentrated to specific membrane domains or structures such as rafts or synaptic vesicles.

In summary, our results here provide novel insights about how plasmalogens bilayers differ from the POPC bilayer and, especially, what role the vinyl–ether linkage plays in this. In the future, the lipid models simulated here can be utilized e.g. in the studies of peptide binding, membrane protein function and lipid membrane fusion.

Author contributions

TR contributed to force field parametrization, analysis, and writing. AK designed the study, run the simulations, carried out the analysis, and wrote the paper.

Conflict of interest

Authors do not have any conflict interests regarding the study.

Acknowledgements

AK has received funding from the European Union´s Seventh Framework Programme for research, technological development and demonstration under grant agreement no. 601055 (VPH-DARE@IT), the Academy of Finland (Centre of Excellence program, project no. 272130 (TR), and the European Research Council (Advanced Grant CROWDED-Pro-LIPIDS (TR)).

References

[1] L.A. Horrocks, M. Sharma, Chapter 2 plasmalogens and O-alkyl glycerophospholipids, New Compr. Biochem. 4 (1982) 51–93.
[2] N.E. Braverman, A.B. Moser, Functions of plasmalogen lipids in health and disease, Biochim. Biophys. Acta (BBA)—Mol. Basis Dis. 1822 (2012) 1442–1452.
[3] X. Han, D.M. Holtzman, D.W. McKeel, Plasmalogen deficiency in early Alzheimer's disease subjects and in animal models: molecular characterization using electrospray ionization mass spectrometry, J. Neurochem. 77 (2001) 1168–1180.
[4] M. Honsho, Y. Yagita, N. Kinoshita, Y. Fujiki, Isolation and characterization of mutant animal cell line defective in alkyl-dihydroxyacetonephosphate synthase: localization and transport of plasmalogens to post-Golgi compartments, Biochim. Biophys. Acta 1783 (2008) 1857–1865.
[5] P. Brites, H.R. Waterham, R.J.A. Wanders, Functions and biosynthesis of plasmalogens in health and disease, Biochim. Biophys. Acta 1636 (2004) 219–231.
[6] L. Ginsberg, S. Rafique, J.H. Xuereb, S.I. Rapoport, N.L. Gershfeld, Disease and anatomic specificity of ethanolamine plasmalogen deficiency in Alzheimer's disease brain, Brain Res. 698 (1995) 223–226.
[7] K. Lohner, A. Hermetter, F. Paltauf, Phase behavior of ethanolamine plasmalogen, Chem. Phys. Lipids 34 (1984) 163–170.
[8] K. Lohner, Is the high propensity of ethanolamine plasmalogens to form nonlamellar lipid structures manifested in the properties of biomembranes? Chem. Phys. Lipids 81 (1996) 167–184.
[9] X. Han, R.W. Gross, Nonmonotonic alterations in the fluorescence anisotropy of polar head group labeled fluorophores during the lamellar to hexagonal phase transition of phospholipids, Biophys. J. 63 (1992) 309–316.
[10] A. Hermetter, B. Rainer, E. Ivessa, E. Kalb, J. Loidl, A. Roscher, F. Paltauf, Influence of plasmalogen deficiency on membrane fluidity of human skin fibroblasts: a fluorescence anisotropy study, Biochim. Biophys. Acta Biomembr. 978 (1989) 151–157.
[11] X. Han, R.W. Gross, Plasmenylcholine and phosphatidylcholine membrane bilayers possess distinct conformational motifs, Biochemistry 29 (1990) 4992–4996.
[12] H. Xianlin, R.W. Gross, Plasmenylcholine and phosphatidylcholine membrane bilayers possess distinct conformational motifs, Biochemistry 29 (1990) 4992–4996.
[13] H.H. Mangold, N. Weber, Biosynthesis and biotransformation of ether lipids, Biophys. J. 22 (1987) 789–799.
[14] A.A. Farooqui, L.A. Horrocks, Plasmalogens, phospholipase A_2, and docosahexaenoic acid turnover in brain tissue, J. Mol. Neurosci. 16 (2001) 263–272.
[15] S.A. Bennett, N. Valenzuela, H. Xu, B. Franko, S. Fai, D. Figeys, Using neurolipidomics to identify phospholipid mediators of synaptic (dys) function in Alzheimer's disease, Front. Physiol. 4 (2013).
[16] A. Maciejewski, M. Pasenkiewicz-Gierula, O. Cramariuc, I. Vattulainen, T. Rog, Refined OPLS all-atom force field for saturated phosphatidylcholine bilayers at full hydration, J. Phys. Chem. B 118 (2014) 4571–4581.
[17] W. Kulig, M. Pasenkiewicz-Gierula, T. Rog, Cis and trans unsaturated phosphatidylcholine bilayers: a molecular dynamics simulation study, Chem. Phys. Lipids (2015).
[18] W.L. Jorgensen, J. Chandrasekhar, J.D. Madura, R.W. Impey, M.L. Klein, Comparison of simple potential functions for simulating liquid water, J. Chem. Phys. 79 (1983) 926–935.
[19] U. Essmann, L. Perera, M.L. Berkowitz, T. Darden, H. Lee, L.G. Pedersen, A smooth particle mesh Ewald method, J. Chem. Phys. 103 (1995) 8577–8593.
[20] S. Páll, B. Hess, A flexible algorithm for calculating pair interactions on SIMD architectures, Comput. Phys. Commun. 184 (2013) 2641–2650.
[21] S. Nosé, A unified formulation of the constant temperature molecular dynamics methods, J. Chem. Phys. 81 (1984) 511–519.
[22] W.G. Hoover, Canonical dynamics: equilibrium phase-space distributions, Phys. Rev. A 31 (1985) 1695.
[23] M. Parrinello, A. Rahman, Polymorphic transitions in single crystals: a new molecular dynamics method, J. Appl. Phys. 52 (1981) 7182–7190.
[24] B. Hess, C. Kutzner, D. van der Spoel, E. Lindahl, GROMACS 4: algorithms for highly efficient, load-balanced, and scalable molecular simulation, J. Chem. Theory Comput. 4 (2008) 435–447.
[25] S. Ollila, M.T. Hyvönen, I. Vattulainen, Polyunsaturation in lipid membranes: dynamic properties and lateral pressure profiles, J. Phys. Chem. B 111 (2007) 3139–3150.
[26] J.M. Smaby, A. Hermetter, P.C. Schmid, F. Paltauf, H.L. Brockamn, Packing of ether and ester phospholipids in monolayers. Evidence for hydrogen-bonded water at the sn-1 acyl group of phosphatidylcholines, Biochemistry 22 (1983) 5808–5813.
[27] M.P. Brown, J. Steers, S.W. Hui, P.L. Yeagle, J.R. Silvius, Role of head group structure in the phase behavior of amino phospholipids. 2. Lamellar and nonlamellar phases of unsaturated phosphatidylethanolamine analogs, Biochemistry 25 (1986) 4259–4267.
[28] T.M. Ferreira, F. Coreta-Gomes, O.H.S. Ollila, M.J. Moreno, W.L.C. Vaz, D. Topgaard, Cholesterol and POPC segmental order parameters in lipid membranes: solid state 1 H-13C NMR and MD simulation studies, Phys. Chem. Chem. Phys. 15 (2013) 1976–1989.
[29] X. Han, X. Chen, R.W. Gross, Chemical and magnetic inequivalence of glcyerol protons in individual subclasses of choline glycerophospholipids: implications for subclass-specific changes in membrane conformational states, J. Am. Chem. Soc. 113 (1991) 7104–7109.
[30] H.U. Gally, G. Pluschke, P. Overath, J. Seelig, Structure of *Escheria coli* membranes. Glycerol auxotrophs as a tool for the analysisof the phospholipid head-group region by deuterium magnetic resonance, Biochemistry 20 (1981) 1826–1831.
[31] A. Botan, A. Catte, F. Favela, P. Fuchs, M. Javanainen, W. Kulig, A. Lamberg, S.M. Miettinen, L. Monticelli, J. Määttä, V.S. Oganesyan, S.O.H. Ollila, M. Retegan, H. Santuz, J. Tynkkynen, Towards atomistic resolution of phosphatidylcholine glycerol backbone and choline head group at different ambient conditions. 2015 (ArXiv. Org. arXiv:1309.2131v2).
[32] J. Seelig, N. Waespe-Sarcevic, Molecular order in cis and trans unsaturated phospholipid bilayers, Biochemistry 17 (1978) 3310–3315.
[33] M.B. Lande, J.M. Donovan, M.L. Zeidel, The relationship between membrane fluidity and permeabilities to water, solutes, ammonia, and protons, J. Gen. Physiol. 106 (1995) 67–84.
[34] J.A. Killian, Hydrophobic mismatch between proteins and lipids in membranes, Biochim. Biophys. Acta Rev. Biomembr. 1376 (1998) 401–416.
[35] E. Winkler, F. Kamp, J. Scheuring, A. Ebke, A. Fukumori, H. Steiner, Generation of Alzheimer disease-associated amyloid β42/43 peptide by γ-secretase can be inhibited directly by modulation of membrane thickness, J. Biol. Chem. 287 (2012) 21326–21334.